Charge transport in lightly reduced graphene oxide: A transport energy perspective

R. S. Kajen, N. Chandrasekhar, K. L. Pey, C. Vijila, M. Jaiswal, S. Saravanan, Andrew M. H. Ng, C. P. Wong, and K. P. Loh

Citation: Journal of Applied Physics **113**, 063710 (2013); doi: 10.1063/1.4792042
View online: http://dx.doi.org/10.1063/1.4792042
View Table of Contents: http://scitation.aip.org/content/aip/journal/jap/113/6?ver=pdfcov
Published by the AIP Publishing

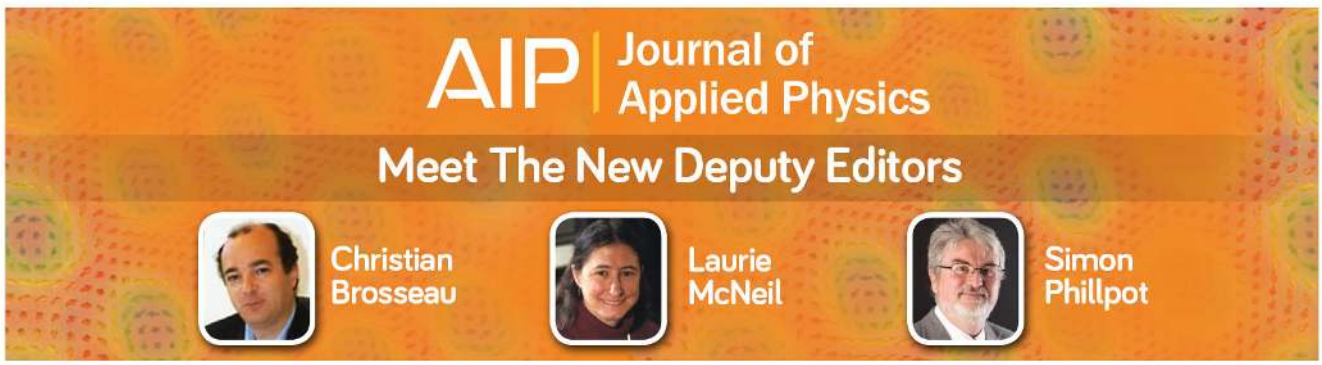

Charge transport in lightly reduced graphene oxide: A transport energy perspective

R. S. Kajen,[1,2] N. Chandrasekhar,[3] K. L. Pey,[2,4,a)] C. Vijila,[1,a)] M. Jaiswal,[5,6] S. Saravanan,[7] Andrew M. H. Ng,[1] C. P. Wong,[8] and K. P. Loh[6]
[1]*Institute of Materials Research and Engineering, A*STAR (Agency for Science, Technology and Research), 3 Research Link, Singapore 117602*
[2]*Division of Microelectronics, School of Electrical and Electronic Engineering, Nanyang Technological University, Singapore 639798*
[3]*19th Cross, Malleswaram, Bangalore 560 055, India*
[4]*Engineering Systems Design, Singapore University of Technology and Design, 20 Dover Drive, Singapore 138682*
[5]*Department of Physics, Indian Institute of Technology-Madras, Chennai 600036, India*
[6]*Graphene Research Center and Department of Chemistry, National University of Singapore, 3 Science Drive 3, Singapore 117543*
[7]*Tera-Barrier Films Pte Ltd, 3, Research Link, Singapore 117602*
[8]*School of Physical and Mathematical Sciences, Division of Physics and Applied Physics, Nanyang Technological University, 21 Nanyang Link, Singapore 637371*

(Received 29 September 2012; accepted 29 January 2013; published online 14 February 2013)

Significant variation in the charge transport behaviour in graphene oxide (GO) ranging from Schottky to Poole-Frenkel and to space charge limited transport exists. These have been extensively reported in the literature. However, the validity of such conventional charge transport models meant for delocalized carriers, to study charge transport through localised states in GO, a disordered semiconductor is open to question. In this work, we use the concept of transport energy (TE) to model charge transport in lightly reduced GO (RGO) and demonstrate that the TE calculations match well with temperature dependent experimental *I-V* data on RGO. We report on a temperature dependent TE ranging from a few 10 meV to 0.1 eV in slightly reduced GO. Last, we point out that, despite the success of several delocalised charge transport models in estimating barrier heights that resemble the TE level, they remain largely accidental and lack the insight in which the TE concept provides in understanding charge transport in RGO. © *2013 American Institute of Physics*. [http://dx.doi.org/10.1063/1.4792042]

I. INTRODUCTION

There have been several reports on the charge transport mechanism in reduced graphene oxide (RGO), reporting behaviour ranging from Schottky limited[1] to Poole-Frenkel,[2] hopping and tunneling,[3] space charge limited current with exponentially distributed traps (SCLC-EDTs)[4] and percolation.[5] However, there has been no clear consensus on a charge transport model for RGO. Despite several variations existing in the experimental conditions, we believe such diverse behaviour has a fundamental cause. Charge carrier injection and transport in disordered organic semiconductors are very different when compared with conventional inorganic semiconductors.[6,7] Several assumptions made in deriving models for charge transport in inorganic materials may not hold[8] for organic materials. Particularly, the applicability of conventional delocalized band transport models to materials where charge transport is mediated by hopping between localized states remains doubtful. Graphene oxide (GO) is a semi-amorphous material,[9] comprising intact graphene-like sp^2 regions embedded in a sp^3 matrix, where the sp^3 regions act as a charge transport barrier between the highly conductive sp^2 regions. We treat GO as a disordered semiconductor with both energetic and positional disorders. Since as-prepared graphene oxide is known to be highly insulating,[1] it becomes necessary to reduce GO to RGO to perform current-voltage (*I-V*) experiments. In this work, we focus on the charge transport mechanisms in lightly reduced GO, since heavily reduced GO is well known to show band-like transport properties.[3] We use laser irradiation[10–12] and mild thermal heating to form lightly reduced GO (resistance (R) ~ 200 GΩ, compared to as-prepared GO flakes with approximately a few tera Ohms resistance). We measure temperature (12 K–350 K) and field dependent current–voltage (*I-V*) characteristics on RGO and compare our experimental results with transport energy (TE) simulations. The concept of transport energy was introduced by Monroe[13] and has been used extensively to describe charge transport in disordered semiconductors by Arkhipov *et al.*[14] The transport energy level describes an energy level which lies within the bandgap, at which hopping transport between localized states is optimized. The hopping process in the vicinity of the TE could be modelled as a "multiple-trapping and detrapping" type of carrier relaxation with the TE playing the role of the mobility edge.[15]

II. EXPERIMENTAL

A. GO synthesis and atomic force microscopy characterization

Big sized graphene oxide (BSGO) flakes were synthesized using a modified Hummer's method using the recipe in

a)E-mail: peykinleong@sutd.edu.sg and c-vijila@imre.a-star.edu.sg.

Ref. 16. The BSGO sheets were then spin-coated on to a prediced 1 cm × 1 cm Si/SiO_2 substrate (300 nm SiO_2 on Si). To characterize the flakes, an atomic force microscopy (AFM) study was carried out using a multi mode-Digital Instruments system in the tapping mode. Fig. 1(a) presents a 10 μm × 10 μm scan region, which confirms the presence of large flakes (extending beyond the scan limits). To determine the number of layers for the flakes, a line profile was taken along a possible single/double layer region, as shown by the dotted line in Fig. 1(a). The analysis of the line profile as shown in Fig. 1(b) confirms the presence of single/double layers from their respective heights of 1 nm and 2.1 nm, respectively.[17]

B. Device fabrication and Raman characterization

A 100 μl, 4% polymethylmethacrylate (PMMA) (MicroChem, MW: 495 K) anisole solution was spin coated on Si/SiO_2 (300 nm) substrates at 4000 rpm and baked at 120 °C for 2 min. The source/drain electrodes were patterned by electron beam (E-beam) lithography (FEI/Sirion), and this was followed by the development of PMMA with a methyl isobutylketone (MIBK) and isopropyl alcohol (1:1) solution. After development, thermal evaporation of 5 nm Cr/35 nm Au was performed in vacuum at 10^{-5} Pa. The sample was then left in acetone overnight before performing liftoff. The samples were then blown dry with N_2. A second E-beam step was used to pattern the etch mask, followed by oxygen plasma (20 W, 20 sccm oxygen plasma (RIE NTI-2312) for 40 s) to etch away the unwanted GO areas. After the final etch step, the sample was left overnight in acetone to remove the resist. Thereafter the samples were cleaned with isopropyl alcohol (IPA) and blown dry with N_2. The inset of Fig. 2 shows the microscope image of a typical GO device with electrodes (yellow) isolated from one another by etched GO-free areas (purple).

Raman spectroscopy was carried out to select the devices with GO in the active device region, using a 488 nm laser of spot size 0.5 μm. Devices with GO gave strong D (1350 cm^{-1}) and G peaks (1600 cm^{-1}) as shown in Fig. 2.[18] The presence of the 2D peak ~ 2700 cm^{-1} corresponds to the presence of unreduced/intact sp^2 regions. The electrodes were wire-bonded after gluing the sample with silver paint to the chip carrier, which was subsequently mounted on a chip socket and placed in a cryostat (Janis-model CCS-450 K) for measurement. The temperature in the cryostat was monitored by a Lakeshore 331 controller. *I-V* measurements were performed using a Keithley femto-ammeter (model-6430) with a remote preamplifier. The electrical measurements were taken in the dark by covering all apertures of the cryostat with aluminium foil. Within the cryostat, the samples were shielded using radiation and vacuum shrouds.

C. Reduction of GO

To reduce GO, the fabricated GO device was irradiated using a 1 mW, 630–670 nm solid state laser, with a spot size of 1 mm, for 1 min. Laser irradiation is known to induce local heating of GO and hence reduce the material.[10–12] After irradiation, the resistance of the material had dropped from T-Ω to approximately 200 G-Ω. The sample was heated at 423 K for 2 h thereafter to further reduce the sample resistance before carrying out the *I-V* experiment. However, the decrease in the sample resistance after the treatment at 423 K was negligible compared to the decrease caused by the laser irradiation. All measurements were repeated several times on several devices to ensure repeatability and consistency.

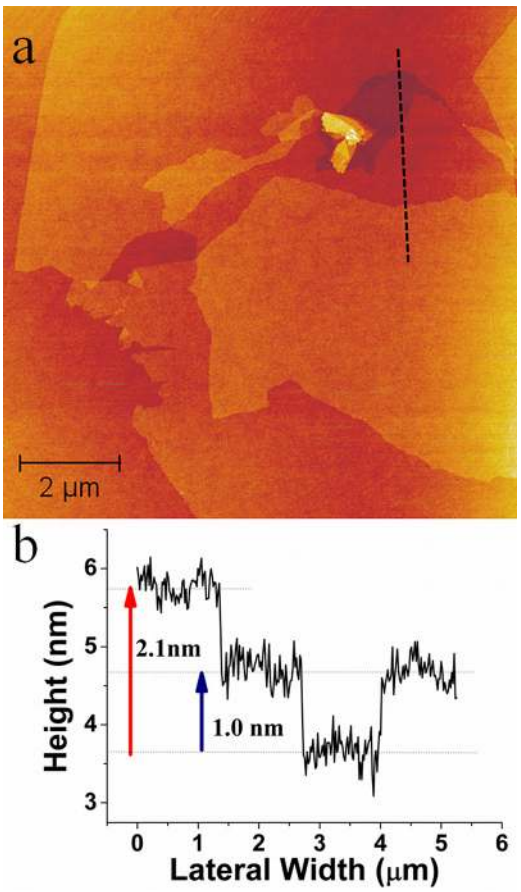

FIG. 1. (a) AFM image of GO. It is clear that the lateral sizes are much larger than the scanning range of the AFM (10 μm in our case). (b) AFM line profile of the dotted line in (a) confirms the presence[17] of both single layer and double layer GO given by their respective thicknesses of 1 nm and 2.1 nm.

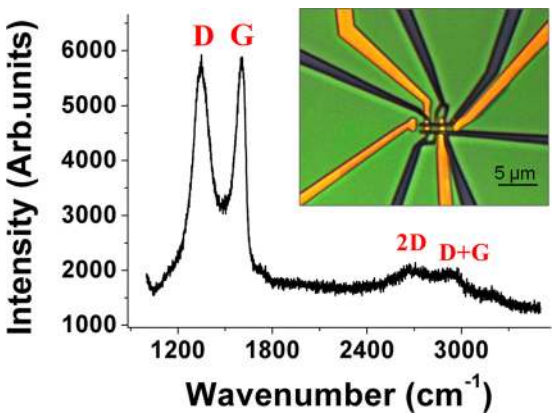

FIG. 2. Plot of Raman intensity versus shift for a representative BSGO sample. The strong D and G peaks confirm the presence of GO. The inset shows the microscope image of a typical GO device with electrodes (yellow) isolated from one another by etched GO-free areas (purple).

III. RESULTS AND DISCUSSION

One of the important questions to answer in charge transport analysis is whether the transport is bulk limited or injection limited. To answer this question, the *I-V* characteristics shown in Fig. 3 are typically fit to various injection-limited models such as the Schottky/ Fowler-Nordheim (F-N) tunneling models or bulk limited models like the Poole-Frenkel or space charge limited conduction.[19]

Fig. 3 depicts the *I-V* characteristics at various temperatures ranging from 12 K to 350 K. While the *I-V* characteristics appear to be symmetric, it remains inconclusive on whether electron or hole transport is predominant, since similar contacts have been used as electrodes. There appears to be little temperature dependence below 110 K (as seen in the inset of Fig. 3) suggesting the presence of tunneling processes dominating charge transport below 110 K. This then gives us a rough estimate of approximately 10 meV (k_BT) for the thermal activation energy in RGO. In the following discussions, we consider the contributions to the current from all possible mechanisms over the range of temperatures investigated.

A. Schottky/Poole Frenkel models

If the energy of the electrons is large enough to launch them across the metal-semiconductor or metal/insulator Schottky barrier, the Schottky current due to such electrons could be modelled using the Schottky current formula

$$J = \frac{4\pi m^* q k_B^2 T^2}{h^3} \exp\left(-\frac{q\phi}{k_B T}\right) \exp\left(\frac{q}{k_B T}\sqrt{\frac{qE}{4\pi\varepsilon_0\varepsilon_r}}\right), \quad (1)$$

where m^* is the effective mass of the electron, $q\phi$ the barrier height, E the applied electric field, ε_0 the vacuum dielectric permittivity, ε_r the relative permittivity of the semiconductor, k_B is Boltzmann's constant, and h is Planck's constant. A popular model used in the presence of traps is the Poole-Frenkel (PF) model which describes field enhanced thermal excitation of trapped electrons into the conduction band as

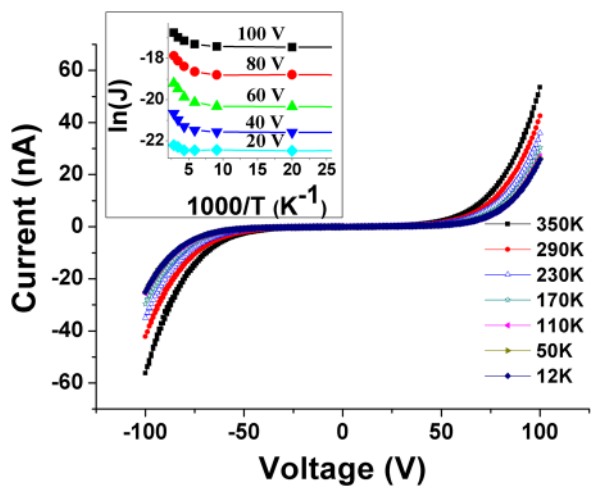

FIG. 3. Temperature dependent *I-V* characteristics of RGO. The inset shows temperature dependence of the current density at 20 V (bottom) to 100 V (top) (in increment of 20 V).

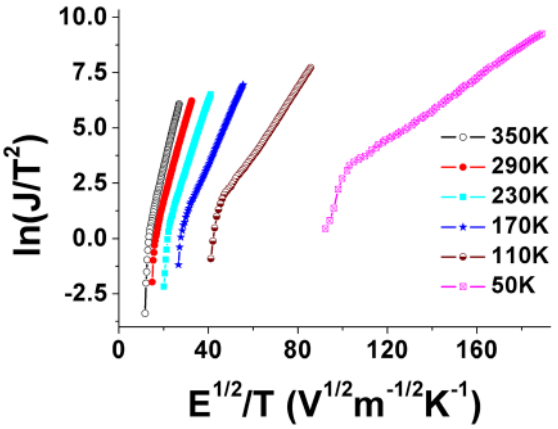

FIG. 4. Schottky plots of temperature dependent *I-V* data shown in Fig. 3.

$$J = q \cdot N_c \cdot \mu_e \cdot E \cdot \exp\left(-\frac{q\phi}{k_B T}\right) \cdot \exp\left(\sqrt{\frac{q}{\pi \cdot \varepsilon_0 \varepsilon_r}}\frac{q\sqrt{E}}{k_B T}\right), \quad (2)$$

where N_C is the density of states (DOS) in the conduction band and μ_e is the electron charge mobility. A similar formula could be also used for hole traps. We next analyze results from the various fits. Figures 4 and 5 show the Schottky and the Poole-Frenkel characteristics, respectively.

Both models appear to fit reasonably well with our data, particularly in the region of moderate to higher fields. However, considerable deviations exist at low fields and low temperatures. This can be discerned as a knee in the Schottky fits and as increasing deviations/noise from the Poole-Frenkel fit. Therefore, we believe that such fits, when observed, have been accidental, for the following reasons. From the experimental and theoretical DOS of GO,[9,21] we know that the electron/hole barrier to the lowest unoccupied/highest occupied molecular orbital (LUMO/HOMO) is at least 2 eV from the Fermi energy. This makes it highly unlikely for the conventional Schottky thermionic emission into the GO HOMO/LUMO as the operating mechanism for charge transport, especially in the absence of gating. None of our devices has a gate. Furthermore, the extracted relative dielectric constant of 1.41 from the Schottky plot (Fig. 4) is

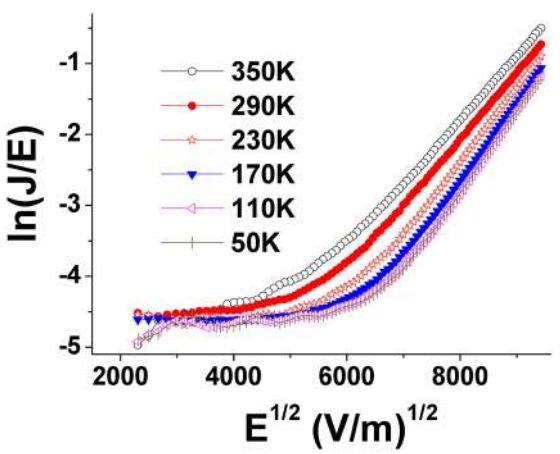

FIG. 5. Poole-Frenkel plots of temperature dependent *I-V* data shown in Fig. 3.

much lower than that found in the literature (between 3 and 12).[1,2,22,23] A subtle point is that under weak temperature dependence, the Schottky plot essentially becomes equivalent to a ln J versus $E^{1/2}$ plot. This type of Poole-Frenkel-like behaviour involving square root field dependence is observed in disordered semiconductors.[24] It has been attributed to field dependent barrier lowering for upward hops in the presence of energetic disorder. Horowitz had also given a similar interpretation for the origin of the PF-like behaviour, due to modification of the Coulombic potential near localized states, leading to an increase in the tunnel transfer rate between sites.[25] Similarly, although the data appears to fit well with the Poole-Frenkel mechanism in Fig. 5, the extracted temperature dependent dielectric constants are within acceptable range only at 290 K and 350 K (below 11). At lower temperatures (31 at 170 K), the dielectric constants become large. Furthermore, the curvature of the Poole-Frenkel plots and the plateau at low fields accompanied by noise indicates that this model is inappropriate. Hence, this suggests that although a ln J versus $E^{1/2}$ relationship exists over a limited range of experimental parameters, the Poole-Frenkel mechanism is not suitable for explaining charge transport in RGO.

In disordered materials, the charge injection from the metal to the disordered semiconductor follows a hopping injection[26] process rather than the conventional thermionic injection process. The charge carrier is essentially injected from the metal Fermi level into a localized state in the disordered material, and hops across the material towards the other electrode. We believe that such is also the case for RGO.

B. Space charge limited and Fowler-Nordheim tunneling models

When the injection rate is higher than what the semiconductor/insulator could accommodate, a SCLC arises as

$$J = \frac{8}{9} \cdot \mu \cdot \frac{\varepsilon_0 \varepsilon_r}{d^3} \cdot V^2, \tag{3}$$

where d is the distance between the electrodes. At low fields, the *I-V* is expected to be ohmic. In deriving this Eq. (3), the effect of traps has been neglected. In the presence of exponentially distributed traps (trap states tailing exponentially in the gap),

$$h(E) = \frac{H_t}{E_t} \exp\left(\frac{-E}{E_t}\right), \tag{4}$$

where h(E) is the trap distribution function in energy E, H_t is the trap density, and E_t is the characteristic energy (for detrapping) of the distribution. The space charge limited current density[20] is modified as

$$J = q^{1-l} \mu N \left(\frac{2l+1}{l+1}\right)^{l+1} \left(\frac{l}{l+1} \frac{\varepsilon_s \varepsilon_0}{H_t}\right)^{l} \frac{V^{l+1}}{d^{2l+1}}, \tag{5}$$

where N is the density of states in the valence/conduction band depending on the trap type and the exponent l ($l = T_C/T$, where T_C is the characteristic temperature) is obtained from the gradient of the log I versus log V curve. Upon extraction of T_C, the characteristic trap energy level E_t is obtained from $k_B T_C$. Further manipulation of Eq. (5) leads to

$$J = \left(\frac{\mu N q V}{d}\right) f(l) \exp\left[-\frac{E_t}{k_B T} \ln\left(\frac{q H_t d^2}{2\varepsilon_s \varepsilon_0 V}\right)\right], \tag{6}$$

where

$$f(l) = \left(\frac{2l+1}{l+1}\right)^{l+1} \left(\frac{1}{l+1}\right)^{l} \frac{1}{2^l}; \tag{7}$$

the function f(l) could be approximated as 0.5 for $l > 2$, hence giving

$$J = \left(\frac{\mu_P N_V q V}{2d}\right) \exp\left[-\frac{E_t}{k_B T} \ln\left(\frac{q H_t d^2}{2\varepsilon_s \varepsilon_0 V}\right)\right]. \tag{8}$$

The trap density could be calculated from ln J versus 1/T plots. An alternative method relies on observing that at a cross-over voltage V_C, the ln term tends to zero giving a temperature independent current. V_C could be extracted by extrapolating the log I versus log V curves at different temperatures. The point, at which the different curves meet, will be the cross-over voltage. Thereafter, the trap density H_t could be calculated using the following equation:

$$V_c = \frac{q H_t d^2}{2\varepsilon_s \varepsilon_0}. \tag{9}$$

From Fig. 6, we observe a deviation between the forward and backward sweep/hysteresis, indicating the presence of charge trapping in RGO. After an initial ohmic region (backward sweep), the log I-log V curve approaches the SCLC-EDT regime where the slope m (the exponent ($m = l + 1$) of V) in Eq. (5) is larger than 2. We extract m values between 5 and 6 from our temperature dependent

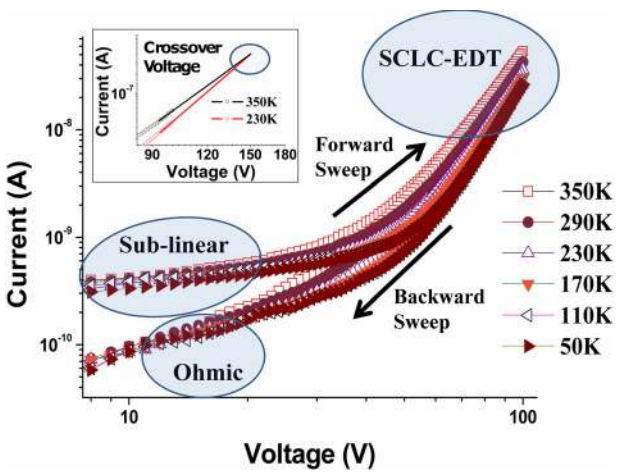

FIG. 6. Temperature dependent log I versus log V characteristics showing hysteresis between upward and downward sweeps due to charge trapping. The oval regions denote the various regimes present/observed: Ohmic, sub-linear (charge trapping), and SCLC-EDT. From the crossover voltage depicted in the inset, the trap density is obtained to be of the order of between 10^{16} and 10^{17} cm^{-3}.

log *I-V* plots. We estimate the trap energy to be 0.123 eV from an m value of 5.9 at 290 K. In addition, from the cross-over voltage of 150 V (see inset of Fig. 6), we estimate the trap density using Eq. (9) to be $6.6 \times 10^{16}\,\mathrm{cm}^{-3}$ assuming a RGO relative dielectric constant of 5. The extracted RGO trap density is in agreement with the trap density found by Joung *et al.*[4] Therefore, any charge transport model has to account for the large density of traps present in GO, leading to the hysteretic behaviour observed above. Although this model can help us to estimate several useful parameters, the mechanism of charge transport in the presence of such a high trap density remains obscured.

An additional possibility exists that the electrons could also tunnel across the barrier depending on the probability. At high applied fields and low temperatures, a FN tunneling current is obtained as

$$J \propto E^2 \exp\left(\frac{-4\sqrt{2m^*}}{3\hbar qE}\left[(q\phi - E_F)^{3/2}\right]\right), \qquad (10)$$

where E_F is the metal Fermi energy level, E is the electric field, and ħ is the reduced Planck's constant. It is clear from the above equations that the Schottky model has very strong temperature dependence, whereas the tunneling model is independent of temperature. From the F-N plots shown in Fig. 7, we obtain a barrier height of 0.127 eV at low temperatures (12 K) and high fields. From Fig. 7, it is also clear that the F-N model is inappropriate, since the fits show curvature rather than the expected straight line.

From the above discussion, it is clear that standard charge transport models used for inorganic semiconductors, rely on band transport, and may at best be of very limited utility to understand the charge transport mechanism in reduced GO, which is a very disordered semiconductor. Bands, as we understand them, do not exist in such materials. Therefore, this requires us to consider a charge transport model developed exclusively for disordered organic semiconductors. The transport energy model is such a model, which we discuss in Sec. III C.

C. Transport energy model

As mentioned earlier, the TE level describes an energy level which lies within the bandgap, at which hopping transport between localized states is optimized. While the conventional models discussed above have generally been intended to describe band transport, we find that the extracted characteristic trap/barrier heights have correlations with the RGO transport energy that cannot be ignored. This motivated us to calculate the TE for RGO. For this calculation, we have followed the procedure of Emelianova *et al.*,[27] using the DOS (g(E)) from Ref. 9 (which has been approximated as a set of triangles for ease of computation), and an inverse localization radius (γ) of $1/6\,\mathrm{nm}^{-1}$ from Ref. 5. The Transport energy (E_{tr}) was computed by solving the following transcendental equation:

$$\int_{-\infty}^{E_{tr}} \frac{(E_{tr} - E)^2\ g(E)}{1 + \exp(-(E - E_F)/k_BT)} dE = \frac{1}{\pi}[2\gamma k_B T]^2. \qquad (11)$$

The results of the calculation are presented in Fig. 8. The transport energy level for electron/hole hopping transport though states with an oxygen atom attached to carbon, and far away from carbon, have been calculated separately as shown in Fig. 8, using the appropriate density of states. The finite temperature (10 K–300 K) thermal filling of localized states has been taken into account in the calculations.

The transport energy depends on temperature since the carrier concentration, charge mobility, and the trapping-detrapping phenomena depend on temperature. While the physical phenomenon is transport through localized states, the effective transport could be, in principle, mapped into a multi-trap and release model, with the transport energy level playing the role of the mobility edge, and the effective "free" carrier density determined by the rate of carrier jumps to/near the effective transport energy level.[7] This then gives a plausible reason for several of the conventional models being invoked for a disordered semiconductor such as GO, and yielding apparently satisfactory agreement, albeit over limited range of experimental parameters. However, fitting alone does not imply that such a charge transport mechanism

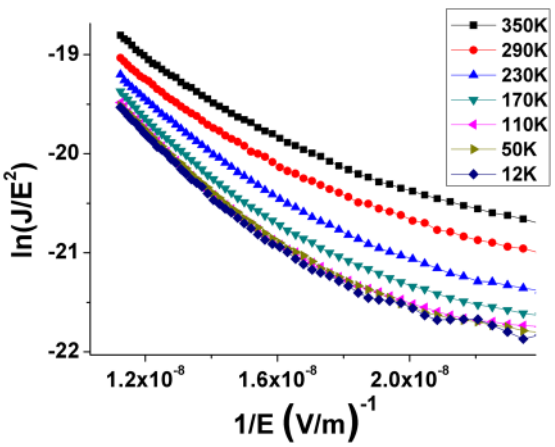

FIG. 7. Temperature dependent FN plots of the *I-V* data shown in Fig. 3.

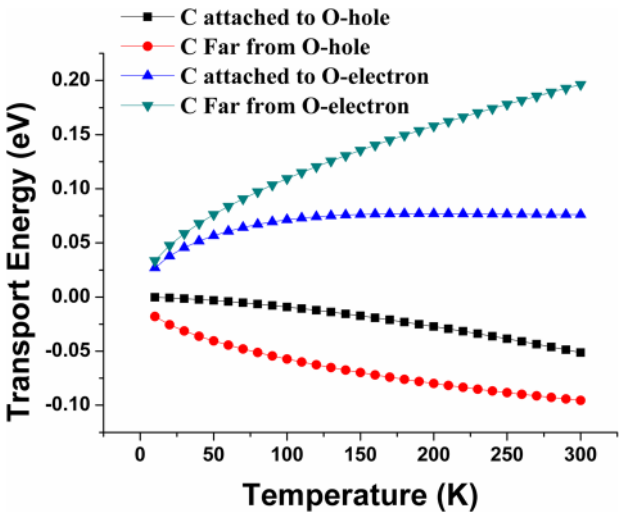

FIG. 8. Transport energy calculation for electrons and holes in RGO for charge transport through states with oxygen attached to the carbon atom and oxygen far away from the carbon atom.

is a valid picture. We compute the hopping current $J_{hopping}$ in RGO using the charge mobility computed from[7,27,28]

$$J_{hopping} = q\mu n_m E, \tag{12}$$

where n_m is the concentration of "mobile carriers" (electrons in this case) which take part in the hopping transport at/above the transport energy. The carrier concentration is calculated by integrating the product of the Fermi-distribution function and the DOS of filled states contributing to the hopping transport near/above the temperature dependent transport energy calculated using Eq. (11). The charge mobility is computed using

$$\mu = D\frac{e}{kTp}\int_{-\infty}^{\infty} dE\ g(E)\frac{\exp\left(\frac{E-E_F}{k_BT}\right)}{\left(1+\exp\left[\frac{E-E_F}{k_BT}\right]\right)^2}, \tag{13}$$

where D is the diffusion coefficient calculated using Eq. (14) (Ref. 28) and p is the total charge carrier density:

$$D = \frac{1}{3}r^2(E_{tr})\nu_0 \exp\left\{-\frac{2r(E_{tr})}{\gamma}\right\}, \tag{14}$$

where $r(E_{tr})$ is the typical hopping distance for electrons at the transport energy E_{tr} and υ_0 is the attempt to escape frequency for hopping between localized states ($10^{13}\,s^{-1}$). The hopping distance is calculated from

$$r(E_{tr}) = \left\{\pi \int_{-\infty}^{E_{tr}} g(E).f(E)\right\}^{-\frac{1}{2}}, \tag{15}$$

where f(E) is the Fermi-Dirac function. We also approximate the impact of backward jumps in reducing the overall hopping current as shown in Fig. 9. We find that the hopping model fits the experimental data extremely well after accounting for a minimum conduction level in RGO, in agreement with work by Kaiser *et al.*[29] Kaiser *et al.* had also postulated the minimum conductance level in RGO to arise from a field-driven hopping mechanism down a potential gradient (without thermal activation but with emission of phonons).[29] While this remains a plausible reason, further simulations and theoretical work need to be carried out to validate the exact origin of the minimum conductance in RGO.

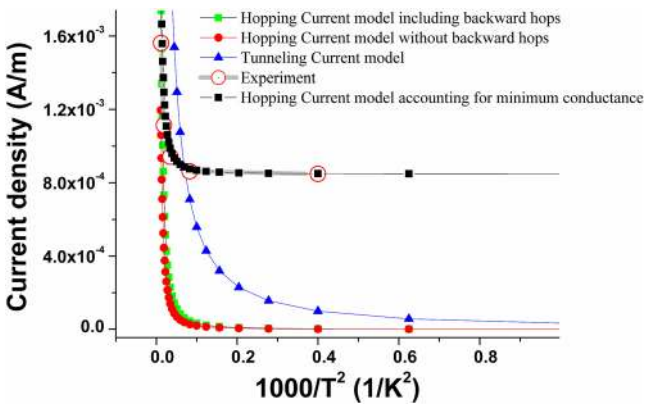

FIG. 9. The experimental curve (red circles with no fill) is compared to hopping models with backward hops (green squares), hopping model without backward hops (red circles), hopping model without backward hops and with a minimum conductance level added (black squares), and a tunneling model (blue triangles) which accounts for the Richardson velocity.

We also compare the hopping model with a tunneling model which takes the temperature dependent Richardson velocity (V_R) into account, as shown in Eq. (16). This equation is valid over a wider range of temperature, in contrast to the FN model which is a low temperature/high field approximation to the general tunneling current across a triangular barrier using the Wentzel–Kramers–Brillouin (WKB) formalism

$$J_{tunneling} = qV_R n\theta, \tag{16}$$

where the tunneling probability θ is given by

$$\theta = \exp\left(-\frac{4}{3}\frac{\sqrt{2qm^*}}{\hbar}\frac{\varphi^{3/2}}{E}\right). \tag{17}$$

Here, q is the electronic charge, m* is taken as the electron rest mass, $\hbar$ is the reduced Planck's constant, φ is the tunneling barrier height taken as 0.127 eV in our simulation, and E is the electric field taken as 35 MV/m in our simulation. The carrier density n is calculated from the DOS in Ref. 9 (again approximated as triangles) and the Fermi-Dirac distribution near the Fermi level of the metal within k_BT, where k_B is the Boltzmann constant and T the temperature in Kelvin. Overall, we find that the hopping model which takes into account a minimum conductivity level and discards backward jumps fits the experimental data best (red circles on a grey line with no fill). From our assessment of various models (linear *I-V*, SCLC-EDT/F-N tunnelling models and transport energy calculations), we conclude that a transport gap of approximately 0.1 eV exists in lightly reduced GO. This gap could be lower, in view of the approximations used in our computations. This is in strong agreement with the work done by Eda *et al.*[3] who show a transport gap of about 50 meV for lightly reduced GO. It is also in agreement with scanning tunneling microscopy (STM) gap measurements on GO by Pandey *et al.*[30] In addition, we also calculate the charge carrier concentration and mobility (using Eq. (13)) in RGO to be $1.3\times10^{11}/8.2\times10^{11}\,cm^{-2}$ and $1.2\times10^{-3}/2.2\times10^{-4}\,cm^2\,V^{-1}\,s^{-1}$ for electrons and holes, at 300 K, respectively.

IV. CONCLUSION

In summary, we have carried out temperature dependent *I-V* measurements of lightly reduced GO using laser irradiation and mild thermal annealing. We explain our results using the concept of transport energy. We model the current through the RGO device and found it to be a function of a minimum conductance level and a temperature and field dependent hopping component. In addition, we demonstrate that although conventional charge transport models used for delocalized band transport tend to fit the *I-V* data reasonably well, they are not representative of the physical phenomena underlying charge transport in RGO. We conclude that such

accidental agreements with conventional models (Schottky, F-N, P-F, etc) arise due to a scenario, whereby the localized hopping transport problem is mapped into a multi-trap and release problem with the transport energy level playing the role of the mobility edge. From transport energy calculations, we found the temperature dependent transport gap to be in the range of a few 10 meV–0.1 eV.

[1]X. Wu, M. Sprinkle, X. Li, F. Ming, C. Berger, and W. A. De Heer, Phys. Rev. Lett. **101**, 026801 (2008).
[2]Y. Kanamori, S. Obataand, and K. Saiki, Chem. Lett. **40**(3), 255 (2011).
[3]G. Eda, C. Mattevi, H. Yamaguchi, H. Kim, and M. Chhowalla, J. Phys. Chem. C **113**, 15768 (2009).
[4]D. Joung, A. Chunder, L. Zhai, and S. I. Khondaker, Appl. Phys. Lett. **97**, 093105 (2010).
[5]C. Mattevi, G. Eda, S. Agnoli, S. Miller, K. A. Mkhoyan, O. Celik, D. Mastrogiovanni, G. Granozzi, E. Garfunkel, and M. Chhowalla, Adv. Funct. Mater. **19**, 2577 (2009).
[6]S. Barth, U. Wolf, H. Bässler, P. Müller, H. Riel, H. Vestweber, P. F. Seidler, and W. Rieß, Phys. Rev. B **60**, 8791 (1999).
[7]V. I. Arkhipov, H. von Seggern, and E. V. Emelianova, Appl. Phys. Lett. **83**, 5074 (2003).
[8]N. Tessler, Y. Preezant, N. Rappaport, and Y. Roichman, Adv. Mater. **21**(27), 2741 (2009).
[9]K. A. Mkhoyan, A. W. Contryman, J. Silcox, D. A. Stewart, G. Eda, C. Mattevi, S. Miller, and M. Chhowalla, Nano Lett. **9**(3), 1058 (2009).
[10]W. Gao, N. Singh, L. Song, Z. Liu, A. L. M. Reddy, L. Ci, R. Vajtai, Q. Zhang, B. Wei, and P. M. Ajayan, Nat. Nanotechnol. **6**, 496 (2011).
[11]Y. Tao, B. Varghese, M. Jaiswal, S. Wang, Z. Zhang, B. Oezyilmaz, K. P. Loh, E. S. Tok, and C. H. Sow, Appl. Phys. A: Mater. Sci. Process. **106**, 523 (2012).
[12]K. P. Loh, Q. Bao, G. Eda, and M. Chhowalla, Nat. Chem. **2**, 1015 (2010).
[13]D. Monroe, Phys. Rev. Lett. **54**, 146 (1985).
[14]V. I. Arkhipov, E. V. Emelianova, and G. J. Adriaenssens, Phys. Rev. B **64**, 125125 (2001).
[15]S. D. Baranovski, *Charge Transport in Disordered Solids with Applications in Electronics* (John Wiley & Sons, England, 2006), p. 69.
[16]S. Wang, P. K. Ang, Z. Wang, A. L. Tang, T. L. Thong, and K. P. Loh, Nano Lett. **10**, 92 (2010).
[17]S. Stankovich, D. A. Dikin, R. D. Piner, K. A. Kohihaas, A. Kleinhammes, Y. Jia, Y. Wu, S. T. Nguyen, and R. S. Ruoff, Carbon **45**, 1558 (2007).
[18]K. N. Kudin, B. Ozbas, H. C. Schniepp, R. K. Prud'homme, I. A. Aksay, and R. Car, Nano Lett. **8**(1), 36 (2008).
[19]H. Bentarzi, *Transport in Metal-Oxide-Semiconductor Structures* (Springer, Berlin, 2011).
[20]V. Kumar, S. C. Jain, A. K. Kapoor, W. Geens, T. Aernauts, J. Poortmans, and R. Mertens, J. Appl. Phys. **92**, 7325 (2002).
[21]T. Bansal, A. D. Mohite, H. M. Shah, C. Galande, A. Srivastava, J. B. Jasinski, P. M. Ajayan, and B. W. Alphenaar, Carbon **50**(3), 808 (2012).
[22]S.-K. Lee, H. Y. Jang, S. Jang, E. Choi, B. H. Hong, J. Lee, S. Park, and J.-H. Ahn, Nano Lett. **12**, 3472 (2012).
[23]G. Eda, P. H. Wöbkenberg, J. Ball, T. D. Anthopoulos, and M. Chhowalla, in Imagine Nano Graphene 2011 Conference Poster Presentation, Bilbao, Spain, 2011.
[24]V. Coropceanu, J. Cornil, D. Filho, Y. Oliver, R. Silbey, and J. Bredas, Chem. Rev. **107**, 926 (2007).
[25]G. Horowitz, Adv. Mater. **10**(5), 365 (1998).
[26]V. I. Arkhipov, E. V. Emelianova, Y. H. Tak, and H. Bassler, J. Appl. Phys. **84**(2), 848 (1998).
[27]E. V. Emelianova, M. van der Auweraer, G. J. Adrianssens, and A. Stesmans, Org. Electron. **9**, 129 (2008).
[28]S. D. Baranovski, M. Zhu, T. Faber, F. Hensel, P. Thomas, M. B. Linden, and W. F. Weg, Phys. Rev. B **55**(24), 16226 (1997).
[29]A. B. Kaiser, C. Gomez-Navarro, R. S. Sundaram, M. Burghard, and K. Kern, Nano Lett. **9**(5), 1787 (2009).
[30]D. Pandey, R. Reifenberger, and R. Piner, Surf. Sci. **602**, 1607 (2008).